DOE/ER/14079--13

DE92 016281

Finite-Difference Migration to Zero Offset

Jianchao Li

Center for Wave Phenomena
Colorado School of Mines
Golden, Colorado 80401
(303) 273-3557

MASTER

DISTRIBUTION OF THIS DOCUMENT IS UNLIMITED

Finite-Difference Migration to Zero Offset

Processed by OSTI
JUN 2 6 1992

Jianchao Li

ABSTRACT

Migration to zero offset (MZO), also called *dip moveout* (DMO) or *prestack partial migration*, transforms prestack offset seismic data into approximate zero-offset data so as to remove reflection point smear and obtain quality stacked results over a range of reflector dips. MZO has become an important step in standard seismic data processing, and a variety of frequency-wavenumber (f-k) and integral MZO algorithms have been used in practice to date.

Here, I present a finite-difference MZO algorithm applied to normal-moveout (NMO)-corrected, common-offset sections. This algorithm employs a traditional poststack 15-degree finite-difference migration algorithm and a special velocity function rather than the true migration velocity. This paper shows results of implementation of this MZO algorithm when velocity varies with depth, and discusses the possibility of applying this algorithm to cases where velocity varies with both depth and horizontal distance.

INTRODUCTION

When reflectors are dipping, common-midpoint (CMP) gathers recorded at the Earth's surface are no longer *common-reflection-point* (CRP) records. The reflections in a CMP gather, in fact, come from different reflection points, a phenomenon called *reflection point smear* or *dispersal*. Although NMO correction can align the reflections that come from horizontal reflectors, it fails to correct those reflections that come from reflectors with a range of dips. As a result, CMP stack after NMO correction will attenuate non-aligned reflections. The reason for this failure, roughly speaking, is that NMO correction is a 1-D process, while reflection-point smear is a 2-D problem; and 1-D processes cannot solve 2-D problems.

One way to ensure CRP stacking of seismic data is the application of full prestack migration (preferably full prestack *depth* migration) to offset data. In principle, this is an ideal way because it can directly position reflections in offset data to their original reflection points. Generally speaking, however, full prestack migration is computationally expensive.

A second approach, which accomplishes CRP stacking in an indirect and approximate manner, consists of four steps: NMO correction, migration to zero offset (MZO), stacking, and poststack migration. The result after the application of these four steps is approximately equivalent to that obtained by using full prestack migration. This approach, in general, is much more practical than full prestack migration.

MZO, also called *dip moveout* (DMO) or *prestack partial migration*, is a key step in the second approach mentioned above. As its name implies, this 2-D prestack process transforms prestack offset data so that they appear like true zero-offset data.

Many papers have been published on the two most commonly used MZO approaches: *frequency-wavenumber* (f-k) MZO and integral MZO (Hale, 1988). In contrast, only a few papers on finite-difference MZO have been published so far. Finite-difference algorithms play an important role in conventional migration methods because they can readily handle velocity variation. Since MZO is a form of migration, finite-difference algorithms should have application there, as well.

Yilmaz and Claerbout (1980) proposed two finite-difference MZO algorithms from analysis of the double square-root equation. Bolondi, et al. (1982) and Salvador and Savelli (1982) presented another finite-difference MZO algorithm, based on the concept of *offset continuation*. These algorithms have generally low efficiency and low accuracy for handling large-offset seismic sections and reflections from steep reflectors.

Here, I present a finite-difference MZO algorithm applied to NMO-corrected common-offset sections. Tests show the effectiveness of this algorithm for handling velocity variations, large offsets, and reflections from steep interfaces.

DERIVATION OF MZO VELOCITY

In constant-velocity media, conventional migration spreads an impulse at the point $(x = 0, t_0)$ in the stacked section to the impulse-response trajectory defined by

$$x^2 + z^2 = (vt_0/2)^2, \tag{1}$$

where x is the CMP coordinate, z is depth, t_0 is zero-offset reflection time, and v is the medium velocity. Equation (1) describes a circle with radius $vt_0/2$ on the x-z plane, the migrated-position domain. If we let $\tau \equiv 2z/v$ denote vertical time, or time-equivalent depth, equation (1) becomes

$$\frac{x^2}{(vt_0/2)^2} + \frac{\tau^2}{t_0^2} = 1. \tag{2}$$

This is an elliptic equation on the x-τ plane, whose two axes are vt_0 and $2t_0$, respectively. That is, the impulse response of conventional migration is a circle on the x-z plane, while it is an ellipse on the x-τ plane.

Now, consider the behavior of MZO. The MZO ellipse, after NMO correction, is defined by

$$\frac{x^2}{h^2} + \frac{t_0^2}{t_n^2} = 1, \tag{3}$$

where t_n is the time after NMO correction, and h is half the source-receiver offset (Hale, 1988). If we define a velocity $\tilde{v}$ such that

$$h \equiv \tilde{v}t_n/2,$$

or

$$\tilde{v} \equiv 2h/t_n, \tag{4}$$

and define a depth quantity

$$\tilde{z} \equiv \tilde{v}t_0/2,$$

then equation (3) becomes

$$x^2 + \tilde{z}^2 = (\tilde{v}t_n/2)^2. \tag{5}$$

defining a circle with radius $\tilde{v}t_n/2$. That is, the impulse response of MZO after NMO correction is an ellipse whose two axes are $2h$ and $2t_n$, respectively, on the x-t_0 plane, while it is a circle on the x-$\tilde{z}$ plane.

Comparing equations (3) and (5) with equations (1) and (2), we find that if the velocity $\tilde{v}$ is used instead of v, then any conventional migration algorithm can be used to perform MZO processing; with this choice, the impulse response of conventional migration is just the MZO ellipse defined by equation (3). I call $\tilde{v}$, defined by equation (4), the MZO *velocity*. Aside from use of a different velocity, the other difference between conventional migration and MZO is that the input to conventional migration is $P(x, t_0)$ and the output is $P(x, \tau)$, while the input to MZO is $P(x, t_n)$ and the output is $P(x, t_0)$. Here, P denotes seismic data.

FINITE-DIFFERENCE MZO

Finite-difference MZO for constant velocity

In the previous section, we defined MZO velocity in constant-velocity media and showed that conventional migration algorithms can be used to perform MZO. Let

us now consider how MZO can be implemented with a traditional poststack, 15-degree finite-difference migration algorithm (Claerbout, 1985). Two reasons for this choice are: (1) among all finite-difference migration schemes, this one has the highest computational efficiency, and (2) examples and analysis in later sections show that, for MZO, this algorithm has sufficient accuracy and ability to handle large-offset data where subsurface reflectors are steep. However, when using a finite-difference algorithm to perform MZO, we must address a practical problem. According to the derivation of MZO velocity, when we compute the response of an impulse at the point (x, t_n), $\tilde{v}$ should be a constant from the time 0 to t_n. This problem, which exists with finite-difference MZO approaches, can be easily and exactly solved in non-recursive integral algorithms, but cannot be exactly solved in finite-difference algorithms, which are recursive processes.

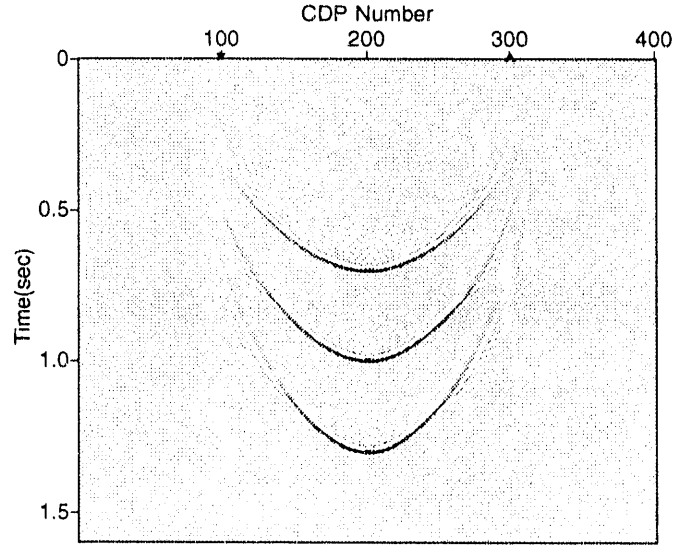

FIG. 1. Impulse responses of finite-difference MZO with velocity $\tilde{v}$. In this test, the CMP interval is 10 m, and offset=2 km.

The impulse responses of finite-difference MZO in Figure 1 show the result of using the velocity defined by equation (4). The distance between the intersections of an impulse response with the surface is greater than $2h$, indicating that the velocity used to obtain this figure is too large. The tests I have done suggest that we can approximately solve this problem by replacing $\tilde{v}$, as given above, by

$$\tilde{\tilde{v}} = 2h/[t_n s(t_0)]. \tag{6}$$

$\tilde{\tilde{v}}$ is the MZO velocity we use in finite-difference MZO under the constant-medium-velocity assumption. I find that when I choose $s(t_0)$ that decreases linearly from about 1.1 at the minimum processing time to 1.0 at the maximum processing time, the impulse responses are squeezed to approximately the correct shapes. With this

slight adjustment of velocity, the finite-difference MZO algorithm can be readily implemented by modifying existing 15-degree finite-difference migration code.

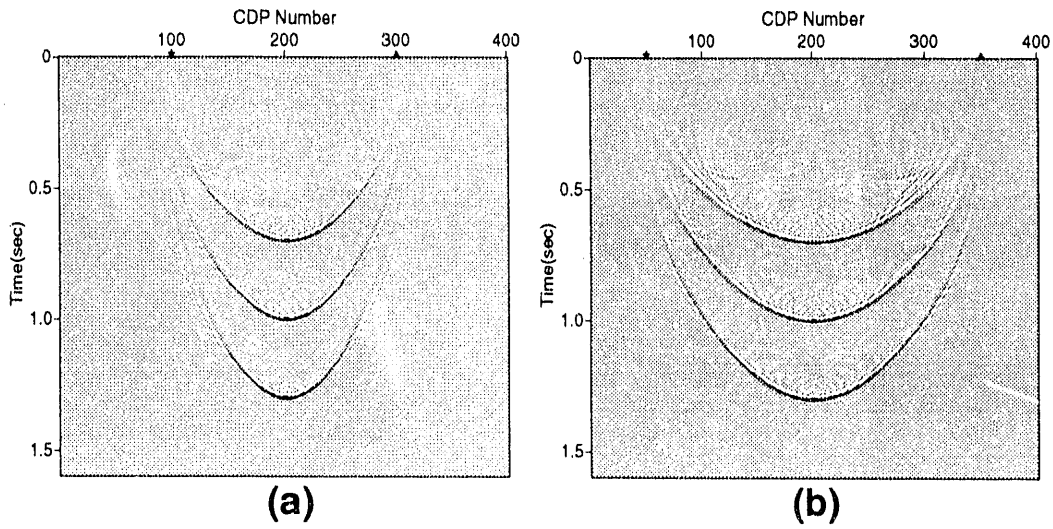

FIG. 2. Impulse responses of finite-difference MZO for constant velocity. In this test, the CMP interval is 10 m. (a) Offset=2 km. (b) Offset=3 km.

Figure 2 shows impulse responses of finite-difference MZO obtained by using the velocity defined by equation (6) with offset of 2 km, in Figure 2a, and 3 km, in Figure 2b. In both the cases, impulse responses are half ellipses and have a tendency to intersect the surface at the shot and receiver points. We sense from this figure that although a so-called 15-degree approximate algorithm is used, we have achieved enough accuracy for both the large offsets and the large dips. These results suggest that when finite-difference algorithms are used to implement conventional migration and MZO, the concept of dip-limited accuracy differs for conventional migration and MZO.

Finite-difference MZO for depth-variable velocity

MZO for depth-variable velocity is often called $V(z)$ MZO. Although velocity variation is often ignored in MZO processing, and constant-velocity MZO processing is often used in areas where velocity is known to vary, many authors (e.g., Hale and Artley, 1991; Artley, 1991; Witte, 1991) have recognized the need to include velocity variation in MZO processing and have attempted to improved the accuracy of MZO approaches when velocity varies with depth. However, generally speaking, it is relatively costly for MZO to handle velocity variations exactly . By introducing Hale's $\gamma(t_n)$ factor (Hale, 1988) in the definition of MZO velocity, we can extend the above finite-difference MZO algorithm so that it can approximately handle velocity variations with depth. Hale (1988) has shown that, for depth-variable velocity, the MZO ellipse defined by equation (3) should be modified as

$$\frac{x^2}{\gamma(t_n)h^2} + \frac{t_0^2}{t_n^2} = 1, \tag{7}$$

where

$$\gamma(t_n) = \frac{3v_4^4(t_n)}{2v_2^4(t_n)} - \frac{t_n}{v_2(t_n)}\frac{dv_2}{dt_n} - \frac{1}{2}, \tag{8}$$

$$v_2(t_n) = [\frac{1}{t_n}\int_0^{t_n} v^2(s)ds]^{1/2},$$

and

$$v_4(t_n) = [\frac{1}{t_n}\int_0^{t_n} v^4(s)ds]^{1/4}.$$

If we define

$$\bar{v} \equiv 2\sqrt{\gamma}h/t_n \tag{9}$$

and

$$\bar{z} \equiv \bar{v}t_0/2,$$

then we obtain

$$x^2 + \bar{z}^2 = (\bar{v}t_n/2)^2 \tag{10}$$

from equation (7). This is also the equation of a circle. Now, we see that the difference between the cases of constant and depth-variable velocity is only in the different definitions of MZO velocity. Moreover, since γ is dependent on t_n only, MZO velocity $\bar{v}$, defined by equation (9), is still a function of t_n, just as is $\tilde{v}$ in the constant-velocity case. So, finite-difference MZO for depth-variable velocity can also be implemented in the same way as in the constant-velocity case. As in equation (6), we also incorporate the $s(t_0)$ factor into the definition of $V(z)$ MZO velocity, equation (9),

$$\bar{\bar{v}} = 2\sqrt{\gamma}h/[t_n s(t_0)]. \tag{11}$$

Finite-difference MZO for (x,z)-variable velocity

$V(x,z)$ MZO, migration to zero offset for (x,z)-variable-velocity media, is a new topic. Van der Schoot, et al. (1989), Popovici (1990), and Hsu (1991) have used modeled traveltime calculation to address this topic. Although the MZO algorithms

discussed above are not theoretically suitable to the laterally variable velocity case, the finite-difference algorithm we adopt provides a possible numerical way for MZO to approximately handle velocity variations in the lateral direction. As is known, neither NMO correction before MZO nor time migration after MZO can exactly deal with laterally variable velocity in theory. In practice, however, these processes handle this issue through lateral interpolation of velocities defined at a number of CMPs in a seismic section and usually can produce acceptable results. For MZO in $v(x, z)$ media with moderate lateral velocity variation, we simply use the $v(z)$ approach developed above with slowly changing velocity along a line, much as is done in conventional NMO and time-migration processing. Since MZO is relatively insensitive to velocity variation, errors in this kind of MZO processing are expected to be smaller than the errors that arise when such a simple approach to lateral variation is taken in NMO correction and time migration.

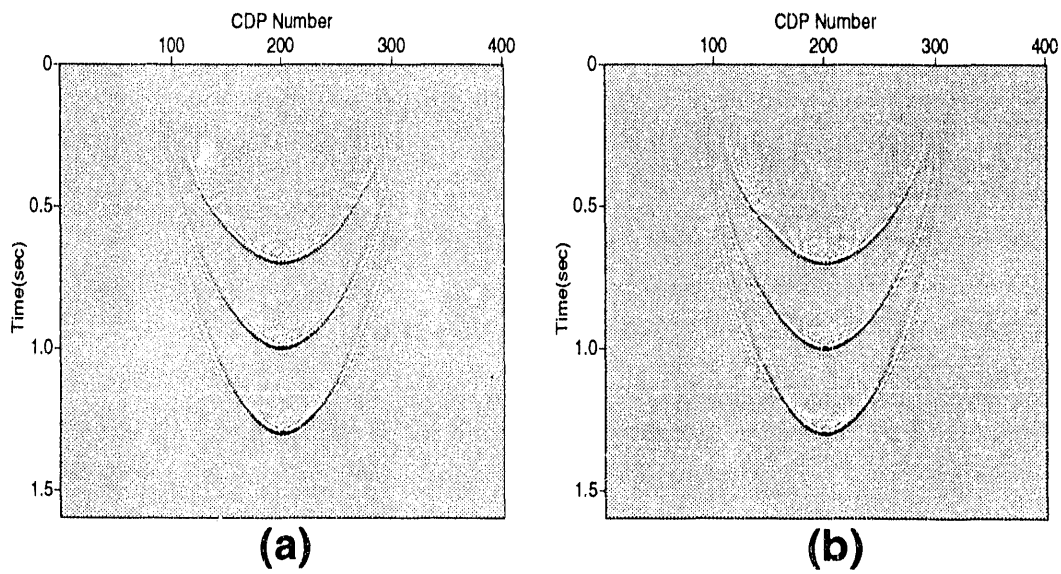

FIG. 3. Impulse responses of finite-difference MZO for (a) the $V(z)$ case and (b) the $V(x, z)$ case. The CMP interval is 10 m.

Figure 3a shows the impulse responses of $V(z)$ MZO for offset= 2 km. In this test, velocity linearly increases from 3 km/s at 0.1 s to 4 km/s at 1.4 s. Comparing Figure 3a with Figure 2a, we see that velocity variation with depth causes the impulse response to narrow slightly. This is consistent with what Hale and Artley (1991) have described. Figure 3b shows the impulse responses of approximate $V(x, z)$ MZO. In this test, I use the same parameters as in Figure 3a, as well as a 0.5 per kilometer linear increase of velocity in the x-direction. We see only minor asymmetry between the left and right branches of the impulse responses in this figure. This suggests that the influence of velocity variation in the lateral direction may not be as significant in MZO as in conventional migration.

SYNTHETIC DATA EXAMPLES

Figure 4 shows a geological model containing nine horizontal reflector segments and five dipping reflector segments, with dips range from 30 to 90 degrees in 15-degree increments. For the synthetic seismic data, the velocity used increases linearly with depth z, according to $v(z) = 1.5 + 0.8z$ km/s, and the CMP interval is 5 m.

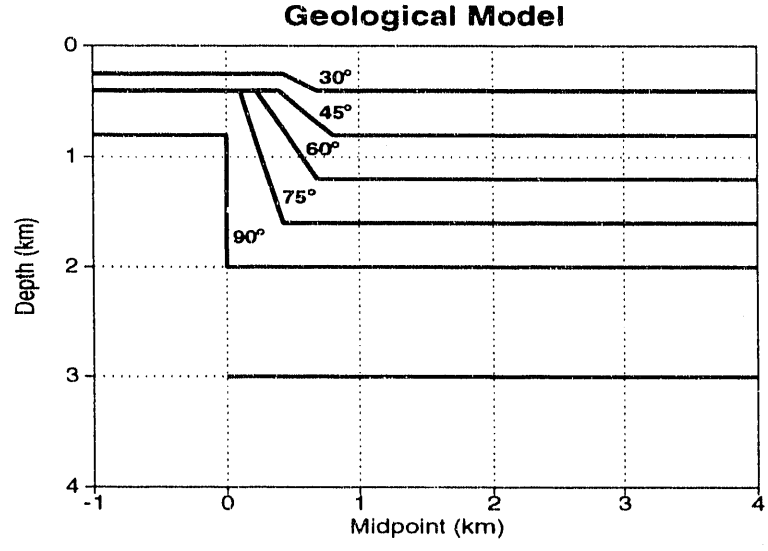

FIG. 4. Geological model used to generate synthetic seismic data.

Four sections obtained after different processings are shown in Figure 5. Figure 5a is a zero-offset synthetic section. The goal of applying MZO is to transform offset data into this form of data. The dashed line in this figure marks the location of the CMP gather shown in Figure 6, and the box shows the region detailed in Figures 5b, 5c and 5d. Figure 5b is a detail of the stacked section obtained by simply stacking ten NMO-corrected common-offset sections, whose offsets range from 0.1 to 1.9 km. We see that the dipping reflections, especially the reflection from the 90-degree reflector, have been attenuated, and some noise, due to out-of-phase stacking, appears among the dipping reflections.

A detail of the stacked result after NMO and constant-velocity MZO corrections is plotted in Figure 5c. Compared with Figure 5b, the stacking quality for dipping reflections in this figure has been significantly improved, but the energy of the dipping reflections is still weaker. Figure 5d shows a detail of the stacked result after NMO and $V(z)$ MZO corrections. In $V(z)$ MZO processing, we used the known *rms* velocity $v_2(t_n)$ for the model. We see from this figure that the stacking quality for dipping reflections, especially the reflection from the 90-degree reflector, has been further significantly improved, and all reflections have amplitudes close to those in the zero-offset section shown in Figure 5a. For comparison, we have used the identical stacking and plotting parameters to get four figures.

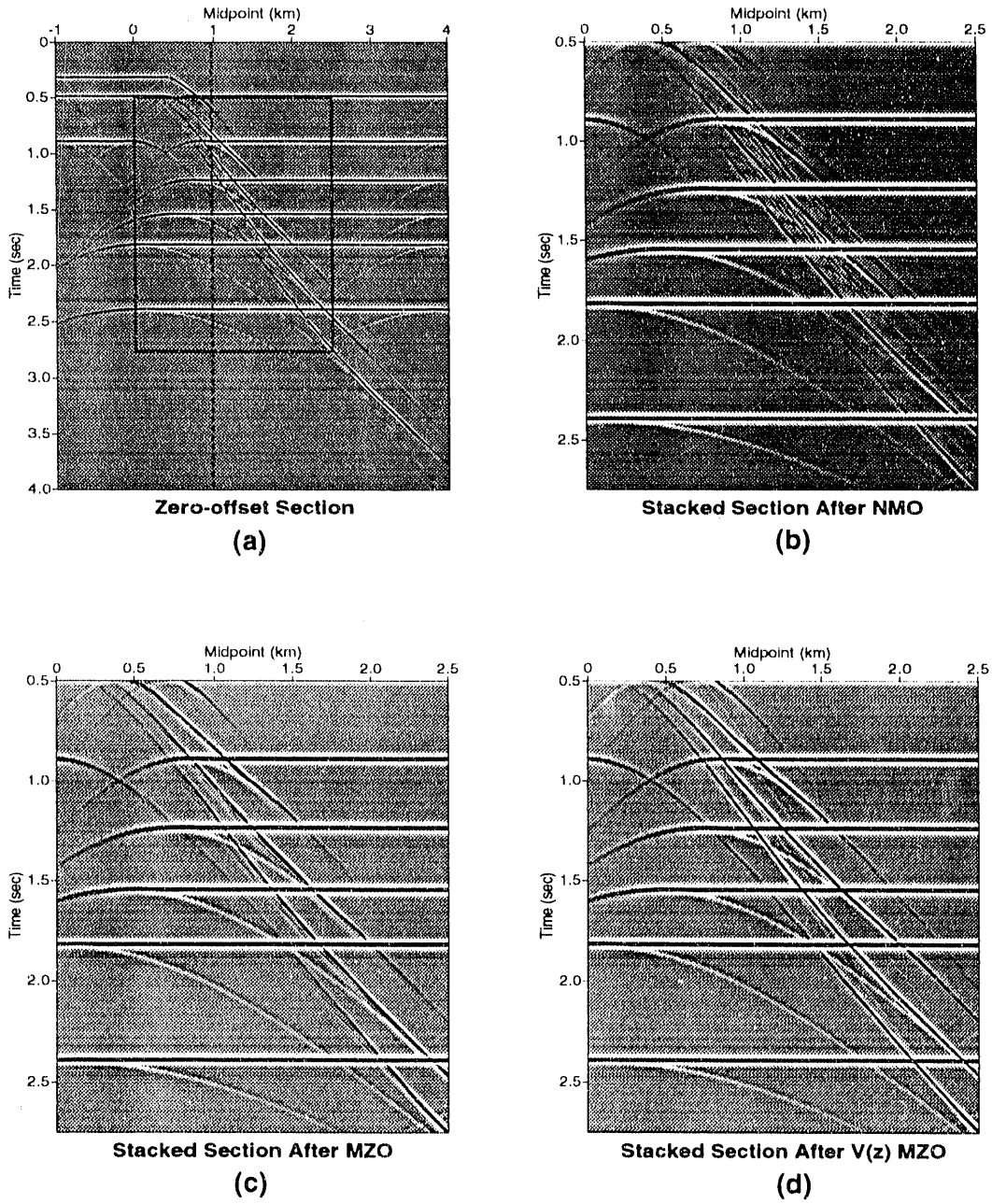

FIG. 5. (a) Zero-offset synthetic section for the geological model shown in Figure 4. The dashed line marks the location of the CMP gather shown in Figure 6. The box shows the location of (b), (c) and (d). (b) Detail of stacked section after NMO correction. (c) Detail of stacked section after NMO and constant-velocity MZO corrections. (d) Detail of stacked section after NMO and $V(z)$ MZO corrections.

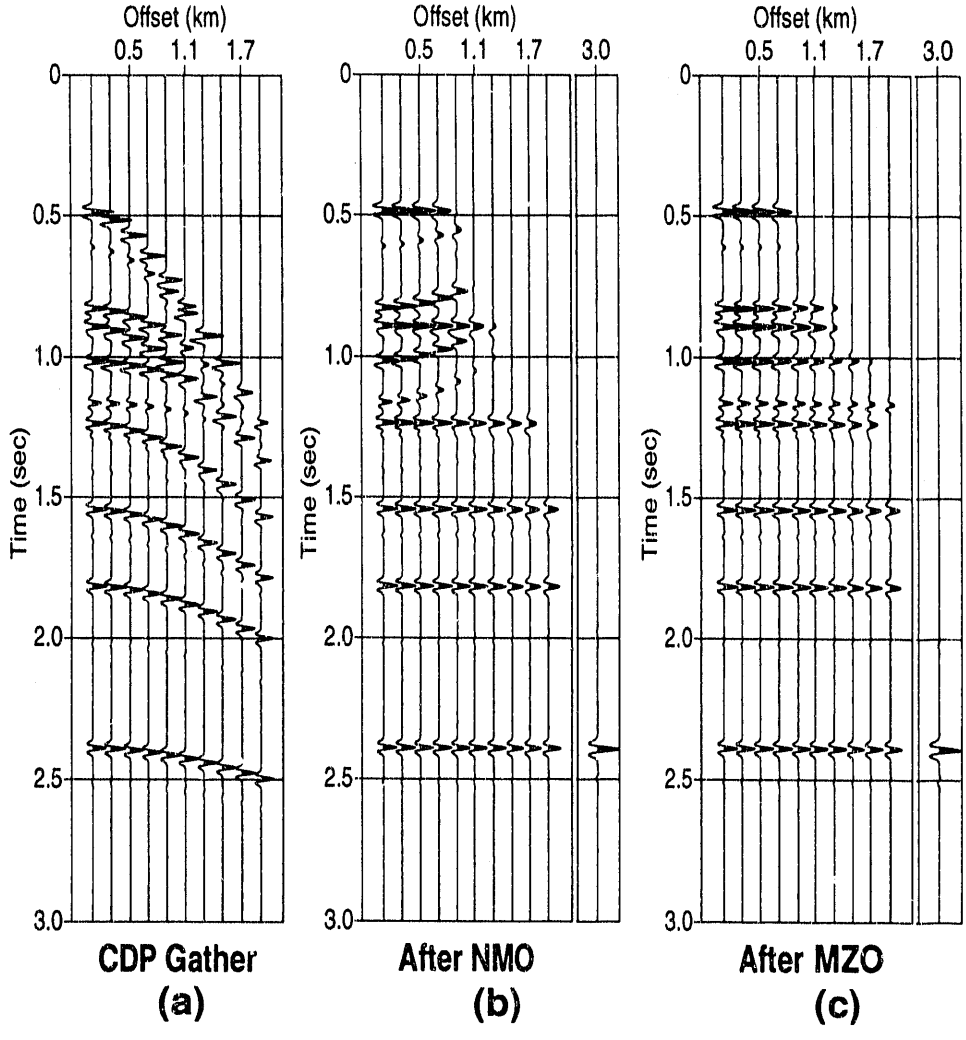

FIG. 6. (a) CMP gather for the model showed in Figure 4. (b) After NMO correction. (c) After $V(z)$ MZO.

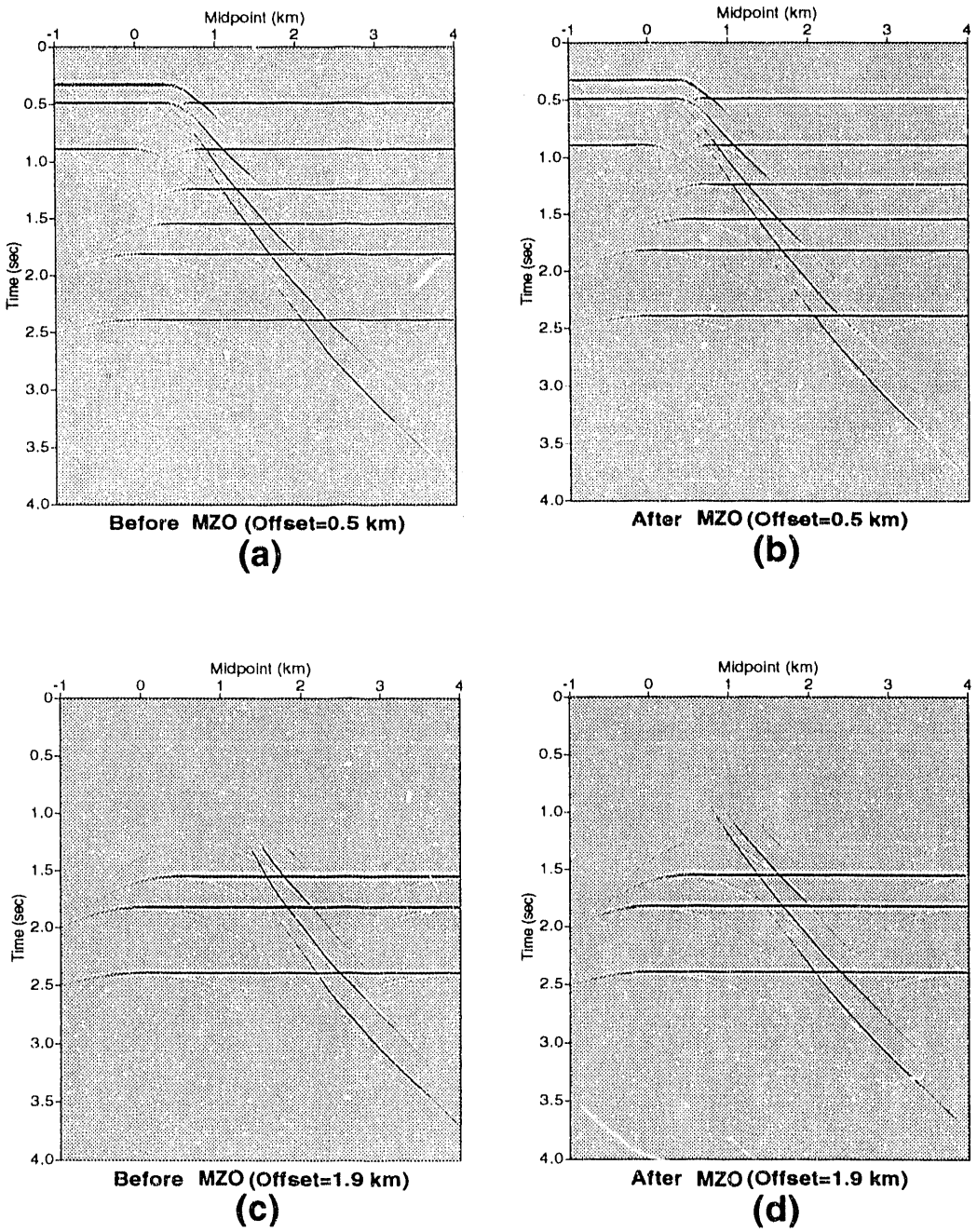

FIG. 7. Comparison among the common-offset sections before and after MZO.

Figure 6 shows the reason why the stacked section after $V(z)$ MZO correction is better than the stacked sections after NMO and constant-velocity MZO corrections. One of the CMP gathers from the model shown in Figure 4 is plotted in Figure 6a. This gather contains six events from horizontal reflectors, five events from dipping reflection segments, and several weak diffraction events from the structural corners. The result of NMO correction applied to the CMP gather of Figure 6a is plotted in Figure 6b. Although the events corresponding to the horizontal reflectors in this gather have been well aligned, some problems appear: (1) the reflections from the dipping reflectors have been over-corrected; (2) the diffractions have also been over-corrected; and (3) anomalously, the event at about 0.6 s corresponding to the 30-degree dipping reflector has amplitude increasing with offset. Obviously, if this NMO-corrected CMP gather is stacked, the poorly aligned events from the dipping reflectors and the diffraction events will be attenuated.

MZO attempts to solve all these problems. Figure 6c shows the result of the finite-difference $V(z)$ MZO correction of Figure 6b. All events that had been over-corrected by NMO in Figure 6b have been aligned back to their "correct" positions with only slightly visible errors, even for the trace with offset of 3 km. As a result, stacking this CMP gather must enhance all events. Furthermore, amplitude values of the event from the 30-degree dipping reflector now decrease with offset, as do those from the other reflectors. In this test, I took the function $s(t_0) = 1.11$ at the minimum processing time. Here, I have not shown the constant-velocity MZO-corrected CMP gather. The constant-velocity MZO did not align all the over-corrected events as well as did the $V(z)$ MZO (Hale and Artley, 1991). So, the stacking quality after the constant-velocity MZO correction is not as good as that after $V(z)$ MZO correction.

Figure 7 offers a comparison among common-offset sections before and after MZO. This figure demonstrates two points: (1) MZO moves dipping reflections only a small amount in both the horizontal and the vertical directions; and (2) although a 15-degree approximate algorithm is used, unlike conventional migration, finite-difference MZO does not generate dispersion or other artifacts even for the reflection corresponding to the 90-degree reflector. These facts again illustrate that the concept of limitation of dips differs for conventional migration and MZO.

CONCLUSION

From the similar kinematics of conventional migration and MZO, I have shown that conventional time migration algorithms, with an approximate choice of MZO velocity, can be used to implement MZO processing. Finite-difference MZO algorithms for constant-velocity and depth-variable velocity have been proposed in this paper, with a suggestion for extending their application to $v(x, z)$ media.

The impulse response tests show the correctness of the finite-difference MZO algorithms. Successful application of finite-difference MZO to synthetic seismic data for a geological model containing steep reflectors, up to 90-degree dip, demonstrates

the effectiveness of finite-difference MZO in handling steep events, large offsets and depth-variable velocity.

Obviously, the finite-difference MZO discussed in this paper is only an approximate method. There are still unsolved problems. For example, finite-difference MZO cannot take into account the two distinct branches of $V(z)$ MZO impulse responses (Artley, 1991). The computational cost of finite-difference MZO is comparable to that of poststack finite-difference migration, but its efficiency is lower than that of f-k MZO.

ACKNOWLEDGEMENTS

Thanks to Dr. Ken Larner for his critical reading and editing of my writing. This work was partially supported by the Consortium at the Center for Wave Phenomena, Colorado School of Mines and by the United States Department of Energy, Grant Number DE-FG02-89ER14079. (This support does not constitute an endorsement by DOE of the views expressed in this paper.)

REFERENCES

Artley, C., 1991, Dip-moveout processing for depth-variable velocity : presented at the 61th Annual International SEG Meeting, Houston, Texas.

Bolondi, G., Loinger, E., and Rocca, F., 1982, Offset continuation of seismic sections: Geophysical Prospecting, **30**, 813-828.

Claerbout, J. F., 1985, Imaging the earth's interior: Blackwell Scientific Publications.

Hale, D., 1988, Dip moveout processing – course notes: Soc. Expl. Geophys.

Hale, D. and Artley, C., 1991, Squeezing dip moveout for depth-variable velocity: **CWP-112**, Colorado School of Mines.

Hsu, Ching-Hsiang, 1991, Kinematics of dip-moveout for variable media: in **CWP-107**, Colorado School of Mines.

Popovici, A. M., 1990, Kinematics of prestack partial migration in variable velocity media: presented at the 60th Annual International SEG Meeting, San Fransico, California.

Salvador, L. and Savelli, S., 1982, Offset continuation for seismic stacking: Geophysical Prospecting, **30**, 829-849.

Van der Schoot, A., Duyndam, A. J., Wapenarr, C. P. A., and Berkhout, A. J., 1989, Common-point-stacking: A macro-model driven approach to DMO: presented at the 59th Annual International SEG Meeting, Dalas, Texas.

Witte, D., 1991, Dip moveout in vertically varying media: presented at the 61th Annual International SEG Meeting, Houston, Texas.

Yilmaz, O. and Claerbout, J. F., 1980, Prestack partial migration: Geophysics, **45**, 1753-1779.

DATE
FILMED
8/27/92